

Original Article



GFT505 Derivatives Ameliorate Alcohol-Induced Hepatic Steatosis and Injury in Vivo and in Vitro

Sule Bai^a, Yi Zou^a, Xiaoxuan Chen^a, Jiajia Yu^a, Futao Liu^a, Zhen Liu^a, Peng Yu^a, Cen Xiang^{a,*}, Yuou Teng^{a,*}

^aChina International Science and Technology Cooperation Base of Food Nutrition/Safety and Medicinal Chemistry, State Key Laboratory of Food Nutrition and Safety, Tianjin University of Science and Technology, Tianjin 300457, China.

*Corresponding Author: Cen Xiang, Yuou Teng

Abstract:

Alcoholic fatty liver disease (AFLD) is a metabolic liver disorder induced by chronic alcohol consumption, characterized by hepatic steatosis, inflammation, and liver injury that may progress to cirrhosis or even hepatocellular carcinoma. Although the PPAR α/δ dual agonist Elafibranor (GFT505) demonstrated metabolic improvement and anti-inflammatory effects in preclinical studies, it failed to achieve expected outcomes in clinical trials. In this study, we identified that its structurally optimized derivative 3a significantly attenuated hepatic lipid accumulation and ameliorated liver injury in both in vitro and in vivo AFLD models, exhibiting promising therapeutic potential. These findings suggest that compound 3a represents a viable drug candidate for AFLD treatment.

Keywords: AFLD; Hepatic lipid accumulation; GFT505 derivative

1. Introduction

Chronic excessive alcohol consumption is a key pathogenic factor in the development and progression of alcoholic liver disease (ALD), with alcoholic fatty liver disease (AFLD) serving as the early pathological stage of ALD¹. Ethanol and its metabolites disrupt hepatic lipid metabolism pathways and impair energy homeostasis, leading to abnormal intracellular lipid accumulation and progressive liver injury. If this pathological process remains uncontrolled, it may progressively develop into liver fibrosis, cirrhosis, and ultimately advance to hepatocellular carcinoma (HCC) or even death²⁻⁵. In the United States, AFLD affects approximately 4.3% of the population and is significantly associated with progression to advanced-stage (F2-F3) hepatic fibrosis. Notably, AFLD-related end-stage liver disease has become one of the leading indications for liver transplantation⁶⁻⁸.

Elafibranor, a first-in-class Peroxisome Proliferator-Activated Receptor α/δ (PPAR α/δ) dual agonist (PPAR α EC₅₀=17 nM; PPAR δ EC₅₀=23 nM), was originally developed by Genfit, Inc^{9, 10}. GFT505 has been clinically demonstrated to ameliorate plasma lipid profiles and insulin resistance in patients with hepatic dysfunction, particularly those with metabolic dysfunction-associated steatotic liver disease (MASLD). Additionally, it reduces systemic inflammatory markers and mitigates liver fibrosis and cirrhosis progression in affected individuals¹¹⁻¹⁴. GFT505 has demonstrated significant therapeutic efficacy in the treatment of primary biliary cholangitis (PBC) and has been approved for clinical use^{15, 16}. However, given the complex pathophysiology of MASLD, a multi-target combination therapy approach may be necessary to achieve satisfactory clinical response rates¹⁷.

In our previous work, we employed a bioisosteric replacement strategy to structurally modify

GFT505, designing and synthesizing a series of novel derivatives. Notably, comparative evaluation revealed that compound **3d** exhibited superior anti-MASH efficacy and reduced cytotoxicity compared to the parent GFT505 molecule (Figure 1)¹⁸. In the present study, we conducted preliminary evaluations of the therapeutic potential of GFT505 derivatives against AFLD in vitro and in vivo. Initially, we employed a HepG2 cell model to evaluate both

the cytotoxicity and therapeutic potential of GFT505 derivatives against AFLD. Preliminary in vitro screening identified derivatives **3a**, **3d**, and **4c** as promising candidates. Subsequent in vivo validation using an AFLD animal model ultimately confirmed that compound **3a** significantly improved lipid metabolism and reduced hepatic injury markers, demonstrating its potential as a therapeutic agent for AFLD.

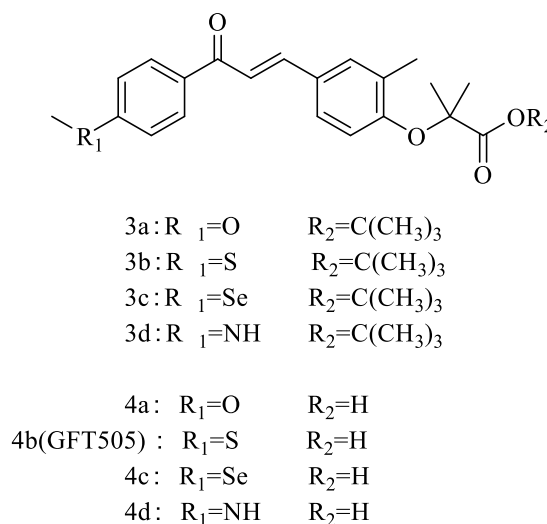


Figure 1. Chemical structures of GFT505 and its derivatives¹⁸

2. Materials and Methods

2.1 Cell Culture

The human hepatocellular carcinoma cell line HepG2 (obtained from the Cell Bank of the Chinese Academy of Sciences, Shanghai, China) was cultured in DMEM medium (Gibco, Beijing, China) supplemented with 10% (v/v) fetal bovine serum (FBS; Cellmax), 1% streptomycin, and 1% penicillin (Gibco, Beijing, China). The cells were maintained in a humidified atmosphere containing 5% CO₂ at 37°C.

2.2 Cytotoxic Activity Assay

The cytotoxicity was evaluated using the MTT (3-(4,5-Dimethyl-2-thiazolyl)-2,5-Diphenyl-2H-tetrazolium bromide, Solarbio, Beijing, China) assay. HepG2 cells were seeded in 96-well plates at a density of 5×10^4 cells/mL and incubated in a constant temperature incubator at 37°C with 5% CO₂ for 24 hours. Subsequently, compound incubation for another 24 hours followed. Then, 20 μL of 0.5% MTT solution was added to the cells and incubated at 37°C for an additional four

hours. After treatment with DMSO for ten minutes, OD values at wavelengths of both 492 nm and 630 nm were measured to calculate cell survival rate. All experiments were conducted in triplicate.

2.3 Oil Red O staining

HepG2 cells were seeded in 6-well plates at a density of 1×10^5 cells/well in 2 mL of culture medium and incubated for 24 h. After incubation, the medium was discarded, and cells were washed three times with PBS (1 mL per wash). Subsequently, 1 mL of serum-free medium was added to each well and incubated for 12 h. DMSO, silymarin (30 μM) and different concentrations of compounds (3, 10, 30 μM) were added to each well and incubated for 24 h. After 24 h, 6-well plates were washed with PBS and fixed in 4% paraformaldehyde for 40 min. Then, oil red O (Solar bio; Beijing; China) was added for staining for 40 min. This was followed by washing with 75% ethanol (v/v) for 10 seconds. The wells were rinsed three times with distilled water and restained with hematoxylin. For each well three images were taken separately and

representative images were shown.

2.4. Intracellular Triglyceride (TG) and Aspartate Transaminase (AST) Assay

HepG2 cells were treated in the same way as in Oil Red O staining. Twenty-four hours after the addition of DMSO, test compounds, or silymarin, the cells were collected and fragmented with cell lysates containing 4% CHAPS. Final tests were performed using TG and AST kits (Nanjing Jianjian Bioengineering Institute; Nanjing; China). Data was normalized by protein content.

2.5 Animal Models

C57BL/6 mice (male, 6 weeks, 18–22 g) were obtained from Beijing Vital River Laboratory Animal Technology Co., Ltd. (Beijing, China). All animal experiments were conducted in accordance with the NIH guide for the care and use of laboratory animals (NIH Publication No. 85-23; revised 1985). The animal procedure has been approved by the Animal Protection Agency Committee of Tianjin University of Science and Technology and strictly adheres to local and national ethical guidelines. The alcoholic fatty liver model of AFLD mice was selected to be induced by Lieber-DeCarli ethanol liquid diet (TP 4030B) fed with Regular type Lieber-DeCarli alcohol liquid model diet provided by Nantong Trofeo Biotechnology Co, Ltd, and the control group Animals were fed with Lieber-DeCarli control liquid diet Lieber-DeCarli control liquid diet (TP 4030C). In the Lieber-DeCarli ethanol liquid diet, the caloric ratios were 35% fat, 19% carbohydrate, and 18% protein, with ethanol providing 28% of the total calories, whereas in the Lieber DeCarli control liquid diet, ethanol's energy supply was completely replaced by carbohydrate, which accounted for 47% of the total calories. All mice were fed ad libitum, without separate drinking water as they were on a liquid chow diet, in a specific pathogen free (SPF) laboratory animal room. In addition, the animal rooms were maintained under light (12-hour light-dark cycle), relative humidity (40-60%), and temperature (20-26°C).

All experimental mice were acclimatized and fed Lieber-DeCarli control liquid chow for 5 days. Subsequently, mice were randomly divided into ethanol-fed model group, control group, positive drug group, compound (3 mg/kg low, 10 mg/kg medium, 30 mg/kg high dose) group and

compound 30 mg/kg high dose control group based on body weight. The control group was given control liquid chow and mice except control and compound control group were given ethanol liquid chow for 4 weeks. After acclimatization feeding the mice were dosed by group and the type of drug administered was selected according to the screening results of the cellular assay for a period of four weeks. After the last administration, the mice were fasted for 12 h. The livers and kidneys were killed, weighed, photographed, and the liver index was calculated as shown in Eq. 1. The blood was collected from the orbital region into a 1.5 mL centrifuge tube, and then centrifuged at 2000 r/min for 10 min after 2 h at room temperature, and then the supernatant was placed in a refrigerator at -80 °C for storage and preparation for the subsequent experimental testing.

$$\text{Liver index (\%)} = \frac{\text{liver weight}}{\text{body weight}} \times 100\% \quad (2-1)$$

2.6. Histological Analysis

Liver tissues were removed immediately after the mice were executed and fixed with 4% paraformaldehyde for 2-3 days. Liver histological analysis was performed and hematoxylin-eosin (H&E) staining was used to assess liver injury, including changes in hepatocyte lipid accumulation, inflammatory cell infiltration and degeneration. Liver samples were embedded in paraffin and processed to prepare 5 µm paraffin sections for H&E staining and oil red O staining.

2.7 Biochemical Analysis

All kits were purchased from Nanjing Bioengineering Research Institute Co., Ltd. and analyzed for serum alanine aminotransferase (ALT), aminotransferase (AST), total cholesterol (TC), and triglyceride (TG) according to the manufacturer's instructions, The results were corrected for their protein content.

2.8 Statistical Analysis

All data were expressed as mean ± standard deviation. The results were analyzed by one-way analysis of variance (ANOVA) and significant differences were determined by Duncan's test using Graph Pad Prism 8.0 (San Diego, CA, USA). $p < 0.05$ was considered as significant.

3. Results

3.1 GFT505 derivatives 3a, 3d, and 4c ameliorate lipid accumulation and suppress AST release in OA- and ethanol-induced AFLD cell model.

The cytotoxicity of **GFT505** and its derivatives was evaluated by MTT assay measuring cell proliferation activity. Figure 2A demonstrates that in the 4s series derivatives containing 2,2-dimethylacetic acid moiety, substitution of the sulfur atom (S) in GFT505 with either oxygen (O, **4a**) or selenium (Se, **4c**) resulted in derivatives exhibiting comparable cytotoxicity to the parent GFT505 compound. However, the NH-substituted compound **4d** did not significantly reduce cell viability even at 30 μM , demonstrating markedly reduced cytotoxicity compared to GFT505. The strategic modification of the acidic terminus with relatively stable and bulky tert-butyl ester groups (**3a-d**) significantly reduced compound cytotoxicity. Notably, the **3a** series demonstrated no observable toxic effects on HepG2 cells across low, medium, and high concentration ranges. These results clearly indicate that **3a-d** derivatives exhibit substantially reduced cytotoxicity compared to the GFT505. As demonstrated by the Oil Red O staining results in Figure 2B, treatment of OA/ethanol-induced AFLD cellular models with 3, 10, and 30 μM GFT505 and its derivatives for 24 hours revealed minimal lipid accumulation in the blank control group, while the model group treated with 0.6% ethanol combined with 1 mM OA showed significant lipid deposition. Notably, all treatment groups receiving 30 μM silymarin or derivatives **3a**, **3d**, and **4a** exhibited marked improvement in intracellular lipid accumulation

compared to the model group.

Triglycerides (TG) and fatty acids are primarily stored in adipocytes through binding with fatty acid synthase (FAS), representing a fundamental mechanism of intracellular lipid storage. Elevated TG levels serve as a key biomarker for AFLD progression¹⁹⁻²¹. As illustrated in Figure 2C, the blank control group exhibited low basal TG content, whereas OA/ethanol co-treatment induced a dramatic increase in cellular TG levels ($P < 0.001$). Silymarin treatment effectively normalized the OA/ethanol-induced hypertriglyceridemia ($P < 0.001$). While GFT505 administration showed no significant effect on cellular TG content, treatment with 10 μM and 30 μM of derivative **3a**, as well as 30 μM of derivatives **3d** and **4a**, significantly ameliorated intracellular TG accumulation ($P < 0.05$).

Elevated aspartate aminotransferase (AST) levels represent a key biomarker of hepatocyte injury²². Figure 2D demonstrates that OA/ethanol co-treatment significantly enhanced AST release in HepG2 cells ($P < 0.001$). Silymarin, GFT505, and derivatives **3a**, **3c**, **3d**, **4a**, **4c**, and **4d** demonstrated significant hepatoprotection through reducing OA/ethanol-induced AST elevation ($P < 0.05$), suggesting their therapeutic potential against alcoholic liver injury.

In summary, derivatives 3a, 3d, and 4a demonstrated significant therapeutic potential for AFLD by effectively ameliorating both lipid accumulation and cellular damage induced by OA/ethanol exposure in the experimental model.

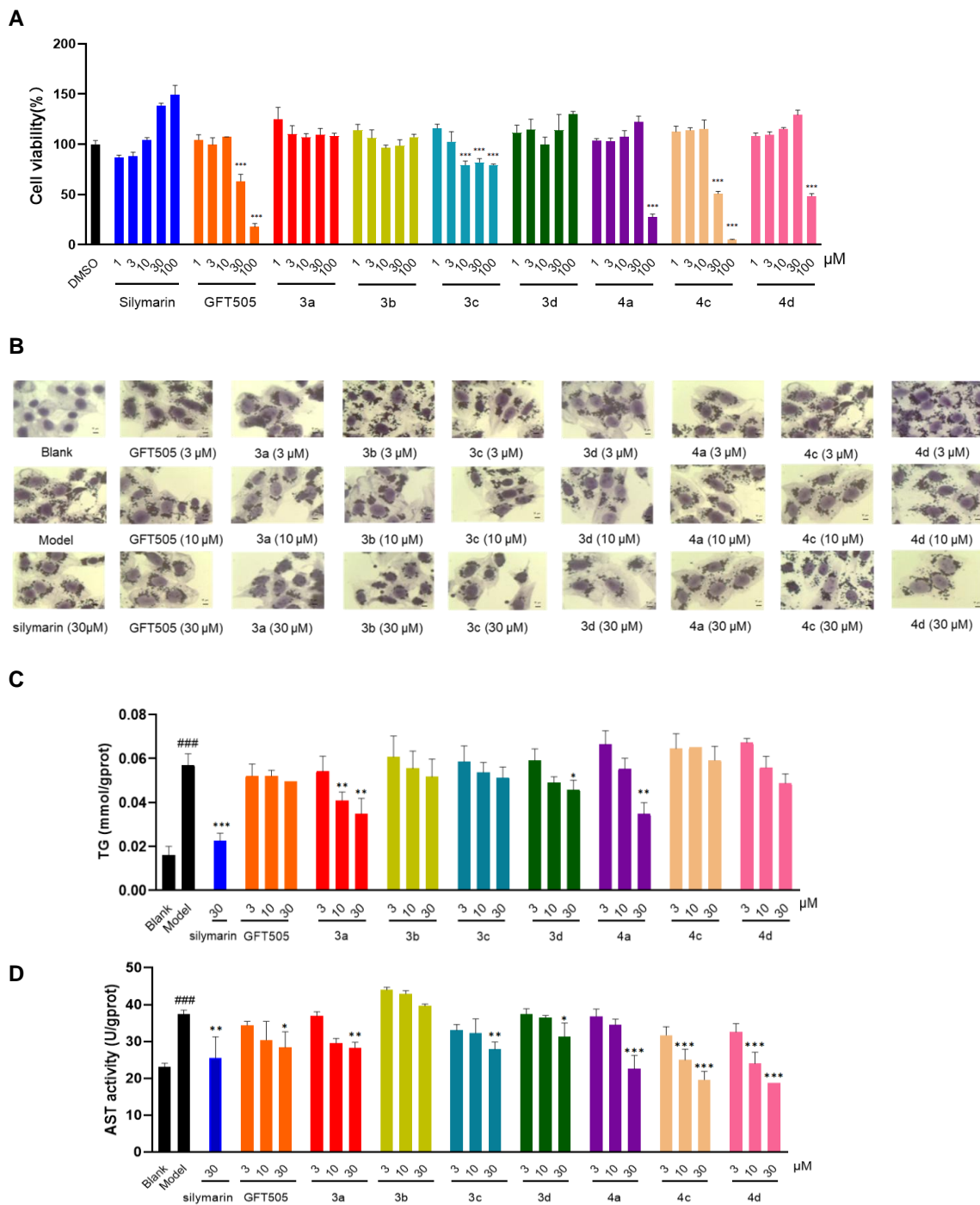


Figure 2. herapeutic effects of compounds 3a, 3d, and 4a in OA/ethanol-induced AFLD cellular model. **A.** Cell viability of HepG2 cells after 24-hour compound treatment. **B.** Oil Red O staining demonstrating attenuation of lipid accumulation $\times 400$, (scale bar=10 μm). **C.** Quantitative analysis of intracellular TG content. **D.** AST release profiles showing hepatoprotective activity. Data represent mean \pm SD, * $p < 0.05$, ** $p < 0.01$, *** $p < 0.001$ vs model.

3.2 Derivatives 3a, 3d, and 4a Ameliorate Lipid Metabolic Disorders in Lieber-DeCarli Diet-Induced AFLD Mice

The liver index in mice serves as a critical indicator of hepatic status. As shown in Figure 3B, while treatment with 4a led to an increase in

the liver index, neither Silymarin nor compounds 3a and 3d significantly altered this parameter. TG, as the most abundant lipid species accumulated in the liver during the progression of fatty liver disease, serve as a critical biomarker for monitoring hepatic steatosis status²³.

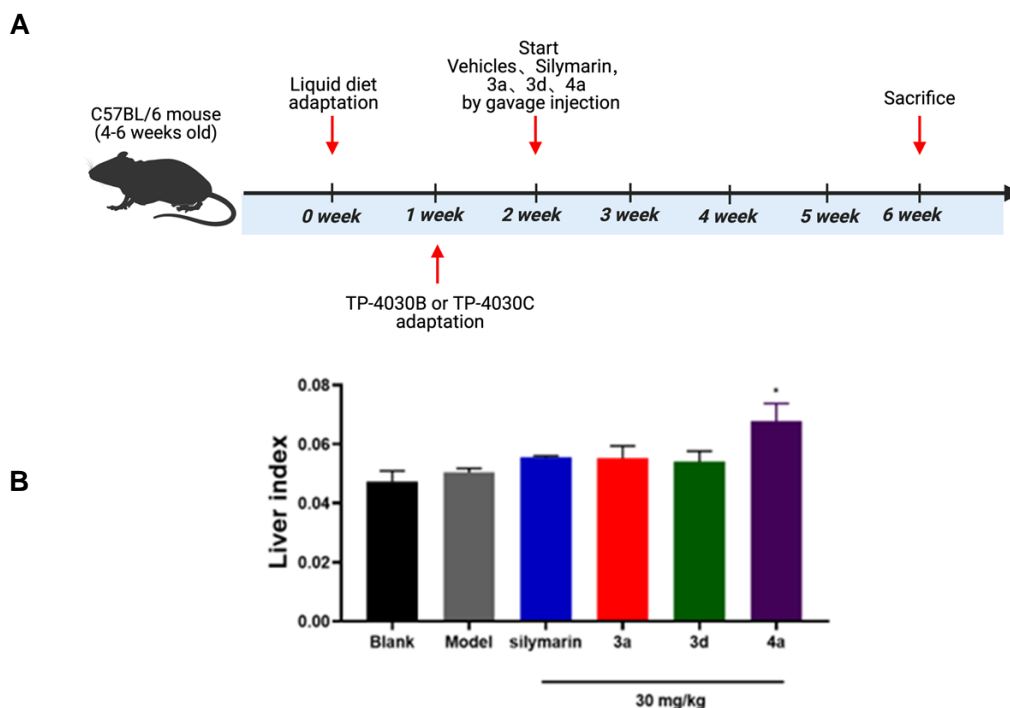


Figure 3. Effects of GFT505 derivatives (3a, 3d, 4a) on liver indices in Lieber-DeCarli diet-induced AFLD mice. A. Establishment of AFLD mouse model. B. Liver indices of AFLD mice after treatment with test compounds. Data presented as mean±SD (n=6). *p<0.05 vs Model.

As shown in Figure 4A, after 4 weeks of treatment with the test compounds in Lieber-DeCarli diet-induced AFLD mice, compared with the model group, both Silymarin (30 mg/kg) and all dose groups of compounds **3a** and **3d** significantly reduced serum TG levels in AFLD mice ($p < 0.05$). Notably, in the **4a** treatment group, significant improvement in serum TG levels was

observed specifically at doses of 10 mg/kg and 30 mg/kg ($p < 0.05$). The liver, as the central organ for cholesterol metabolism, orchestrates the biosynthesis and storage of TC. Serum TC, representing the sum of cholesterol across all lipoprotein particles, serves as a pivotal biomarker for evaluating hepatic lipid metabolic capacity^{24, 25}.

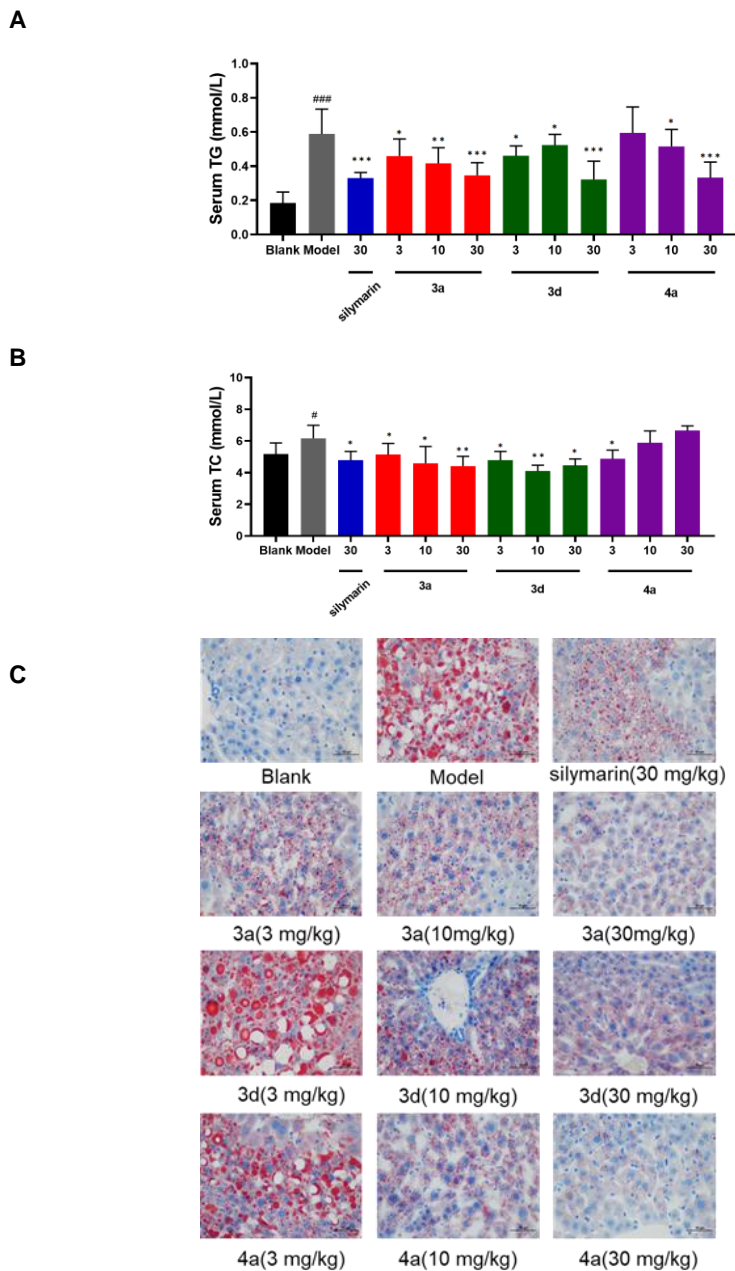


Figure 4. Effects of derivatives **3a**, **3d** and **4a** on lipid accumulation in Lieber-DeCarli diet-induced AFLD mice. **A** Serum TG levels. **B** Serum TC levels. **C** Representative Oil Red O staining of liver tissues original magnification $\times 400$ (scale bar = $50 \mu\text{m}$). Data presented as mean \pm SD ($n=6$). # $p<0.05$, ### $p<0.001$ vs Blank; * $p<0.05$, ** $p<0.01$, *** $p<0.001$ vs Model.

As shown in Figure 4B, treatment with Silymarin, **3a**, or **3d** significantly reduced serum TC levels in mice with Lieber-DeCarli diet-induced AFLD Mice ($p<0.05$), whereas **4a** treatment demonstrated no significant effect on TC levels. Oil Red O staining visually demonstrated progressively fewer lipid droplets in **3a**, **3d**, and **4a** treated groups with increasing doses, with **3a** showing the most pronounced improvement compared to the model group (Figure 4C).

3.3 Ameliorative Effects of Derivatives **3a**, **3d**

and **4a** on Hepatic Pathological Injury in Lieber-DeCarli Diet-Induced AFLD Mice

Subsequently, we further evaluated the therapeutic effects of compounds on hepatic pathology through H&E staining of liver sections. Mice fed with Lieber-DeCarli ethanol diet exhibited characteristic hepatic steatosis and ballooning degeneration. The silymarin treatment group showed marked attenuation of steatosis. Notably, compounds **3a**, **3d** and **4a** demonstrated dose-dependent improvements in histopathology - with increasing doses (3-30 mg/kg), both the number of

steatotic vacuoles and proportion of ballooned hepatocytes were significantly reduced (Figure 5A).

Serum aspartate aminotransferase (AST) and alanine aminotransferase (ALT) serve as crucial biochemical markers for hepatocyte injury. Lieber-DeCarli ethanol diet feeding significantly elevated both ALT and AST activities in the model group ($p < 0.001$ vs Blank). The silymarin only

significantly reduced ALT levels ($p < 0.05$) without improving AST activity. Notably, compounds **3a** and **4a** exhibited dose-dependent dual regulatory effects, concurrently decreasing both ALT and AST levels at doses of 3-30 mg/kg ($p < 0.05$, $p < 0.01$). In contrast, compound **3d** selectively attenuated ALT activity ($p < 0.001$) without significant effects on AST (Figure 5B and 5C).

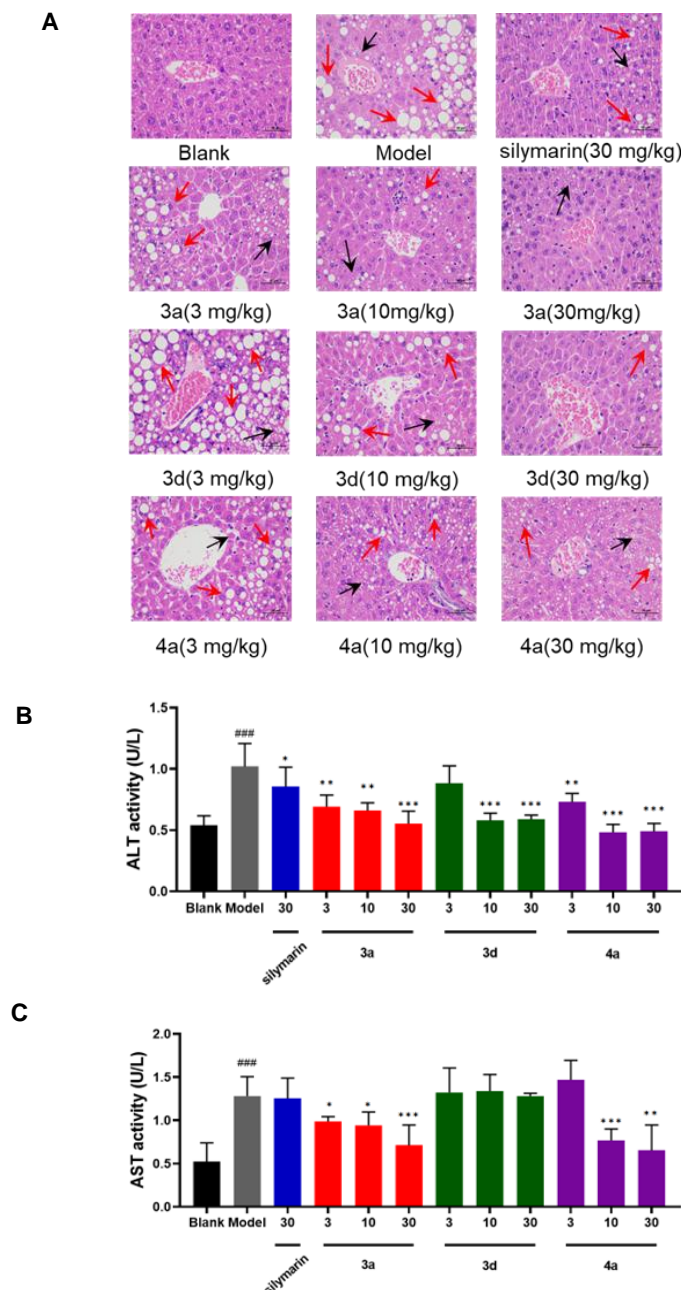


Figure 5. Therapeutic effects of derivatives **3a**, **3d** and **4a** on hepatic pathology in Lieber-DeCarli diet-induced AFLD mice. **A.** Representative H&E-stained liver sections showing steatosis (black arrows) and ballooning degeneration (red arrows) (scale bar=50 μ m). **B.** Serum alanine aminotransferase (ALT) levels. **C.** Serum aspartate aminotransferase (AST) levels. Data are mean \pm SD (n=6). ### $p < 0.001$ vs blank control; * $p < 0.05$, ** $p < 0.01$, *** $p < 0.001$ vs model

4. Conclusion

This study screened eight GFT505 derivatives using an *in vitro* HepG2-based AFLD model, identifying **3a**, **3d** and **4a** as superior to **GFT505** in reducing cellular lipid accumulation. Subsequent *in vivo* studies employed the Lieber-DeCarli diet-induced AFLD mouse model to evaluate therapeutic potential. After 4-week treatment, serum parameters (TC, TG, AST, ALT) and liver histopathology were analyzed. Results showed: **3a** significantly reduced serum TG/TC levels, hepatic lipid deposition, and ALT/AST activities while improving histopathology; **3d** decreased TG/TC and ALT levels with improved histology but unaffected AST; **4a** ameliorated steatosis and lowered ALT/AST but only reduced TG. Notably, **3a** demonstrated the most comprehensive efficacy, suggesting its potential as the optimal GFT505 derivative for AFLD treatment.

In conclusion, our integrated *in vitro* and *in vivo* investigations have systematically evaluated the therapeutic potential of GFT505 derivatives for alcoholic fatty liver disease (AFLD). The HepG2 cell-based screening model identified compounds **3a**, **3d**, and **4a** as showing superior efficacy to **GFT505** in reducing intracellular lipid accumulation ($p < 0.05$). Subsequent evaluation in the Lieber-DeCarli diet-induced AFLD murine model demonstrated that compound **3a** exhibited the most comprehensive therapeutic profile among the tested derivatives, including significant reductions in serum TG and TC levels ($p < 0.01$), normalization of ALT/AST activities ($p < 0.001$), and marked attenuation of hepatic lipid deposition. The outstanding multi-target therapeutic performance of compound **3a**, particularly its dual improvements in both metabolic regulation and hepatoprotection, establishes it as a promising lead candidate for AFLD treatment. These findings collectively confirm that structural optimization represents an effective strategy for developing enhanced GFT505 derivatives with improved therapeutic efficacy against AFLD.

Acknowledgments

The authors gratefully acknowledge the technical support provided by Research Centre of Modern Analytical Technology, Tianjin University of Science & Technology.

Conflicts of Interest

The authors declare no conflicts of interest.

Author contributions

The authors' contributions are as follows: Sule Bai performed experiments, conducted data analysis, and wrote the original manuscript. Yi Zou contributed to manuscript revision and editing. Xiaoxuan Chen carried out animal experiments and cell experiments. Jiajia Yu contributed to research methodology. Futao Liu performed data validation. Peng Yu and Zhen Liu were responsible for project management. Cen Xiang and Yuou Teng oversaw project administration and funding acquisition. All authors reviewed the results and approved the final version of the manuscript.

LIST OF ABBREVIATIONS

ALD = alcoholic liver disease

AFLD = alcoholic fatty liver disease

TG = Triglyceride

TC = Total Cholesterol

H&E staining = hematoxylin and eosin staining

MASLD = Metabolic Dysfunction-Associated Steatotic Liver Disease

MASH = metabolic dysfunction-associated steatohepatitis

OA = Oleic Acid

HCC = Hepatocellular Carcinoma

PPAR = Peroxisome Proliferator Activated Receptor

EC₅₀ = Half-Maximal Effective Concentration

PBC = Primary Biliary Cholangitis

SPF = Specific Pathogen Free

ALT = Alanine Aminotransferase

AST = Aspartate Aminotransferase

DMSO = Dimethyl Sulfoxide

FAS = fatty acid synthase

Funding

This research was funded by Tianjin Science and

Technology Program Project (20YDTPJC00950) and the Natural Science Foundation of China (81703014)

References

- Patel, R. and Mueller, M., Alcoholic Liver Disease. In *StatPearls*, Treasure Island (FL) ineligible companies. Disclosure: Matthew Mueller declares no relevant financial relationships with ineligible companies., 2024.
- Duan, Y., Llorente, C., Lang, S., Brandl, K., Chu, H., Jiang, L., White, R. C., Clarke, T. H., Nguyen, K., Torralba, M., Shao, Y., Liu, J., Hernandez-Morales, A., Lessor, L., Rahman, I. R., Miyamoto, Y., Ly, M., Gao, B., Sun, W., Kiesel, R., Hutmacher, F., Lee, S., Ventura-Cots, M., Bosques-Padilla, F., Verna, E. C., Abraldes, J. G., Brown, R. S., Jr., Vargas, V., Altamirano, J., Caballera, J., Shawcross, D. L., Ho, S. B., Loutch, A., Lucey, M. R., Mathurin, P., Garcia-Tsao, G., Bataller, R., Tu, X. M., Eckmann, L., van der Donk, W. A., Young, R., Lawley, T. D., Starkel, P., Pride, D., Fouts, D. E. and Schnabl, B., Bacteriophage targeting of gut bacterium attenuates alcoholic liver disease. *Nature*, 2019, 575, 505-511.
- Yao, P., Zhang, Z., Liu, H., Jiang, P., Li, W. and Du, W., p53 protects against alcoholic fatty liver disease via ALDH2 inhibition. *EMBO J*, 2023, 42, e112304.
- Smith, A., Baumgartner, K. and Bositis, C., Cirrhosis: Diagnosis and Management. *Am Fam Physician*, 2019, 100, 759-770.
- Zhang, P., Wang, W., Mao, M., Gao, R., Shi, W., Li, D., Calderone, R., Sui, B., Tian, X. and Meng, X., Similarities and Differences: A Comparative Review of the Molecular Mechanisms and Effectors of NAFLD and AFLD. *Front Physiol*, 2021, 12, 710285.
- Wong, T., Dang, K., Ladhani, S., Singal, A. K. and Wong, R. J., Prevalence of Alcoholic Fatty Liver Disease Among Adults in the United States, 2001-2016. *JAMA*, 2019, 321, 1723-1725.
- Videla, L. A., Valenzuela, R., Zuniga-Hernandez, J. and Del Campo, A., Relevant Aspects of Combined Protocols for Prevention of N(M)AFLD and Other Non-Communicable Diseases. *Mol Nutr Food Res*, 2024, 68, e2400062.
- Guohong, L., Qingxi, Z. and Hongyun, W., Characteristics of intestinal bacteria with fatty liver diseases and cirrhosis. *Ann Hepatol*, 2019, 18, 796-803.
- N., H. A., M., K. M., A., T. R., A., A. B., A., H. O., M., E. M., S., E.-K. A. and M., A. Y., Elafibranor modulates ileal macrophage polarization to restore intestinal integrity in NASH: Potential crosstalk between ileal IL-10/STAT3 and hepatic TLR4/NF- κ B axes. *Biomedicine & Pharmacotherapy*, 2023, 157.
- Colin, S., Briand, O., Touche, V., Wouters, K., Baron, M., Pattou, F., Hanf, R., Tailleux, A., Chinetti, G., Staels, B. and Lestavel, S., Activation of intestinal peroxisome proliferator-activated receptor- α increases high-density lipoprotein production. *Eur Heart J*, 2013, 34, 2566-2574.
- Adnan, M., Mahum, N. and Imran, M. M., Efficacy of elafibranor in patients with liver abnormalities especially non-alcoholic steatohepatitis: a systematic review and meta-analysis. *Clinical journal of gastroenterology*, 2021, 14.
- Cariou, B. and Staels, B., GFT505 for the treatment of nonalcoholic steatohepatitis and type 2 diabetes. *Expert Opin Investig Drugs*, 2014, 23, 1441-1448.
- Hanf, R., Millatt, L. J., Cariou, B., Noel, B., Rigou, G., Delataille, P., Daix, V., Hum, D. W. and Staels, B., The dual peroxisome proliferator-activated receptor α /delta agonist GFT505 exerts anti-diabetic effects in db/db mice without peroxisome proliferator-activated receptor γ -associated adverse cardiac effects. *Diab Vasc Dis Res*, 2014, 11, 440-447.
- Pirola, L., Elafibranor, a dual PPAR α and PPAR δ agonist, reduces alcohol-associated liver disease: Lessons from a mouse model. *World J Gastroenterol*, 2025, 31, 99312.
- Nikolaos, P., Konstantinos, S., Michael, F., S, V. S. and S, M. C., Both Elafibranor and Liraglutide Improve NAFLD / NASH but Affect Differentially the Hepatic Lipidome and Metabolome in a Diet-Induced Obese and Biopsy-Confirmed Mouse Model of NASH. *Journal of the Endocrine Society*, 2021, 5.

16. Blair, H. A., Correction: Elafibranor: First Approval. *Drugs*, 2024, 84, 1165.
17. M., S. J., Albert, P., V., K. K., A., H. M., Stephen, C., Daniel, P., Alan, B., M., H. G., Cynthia, L., John, V., David, J., Anne, T., Bart, S., Sophie, M., Remy, H., David, M., Pascal, B. and Velimir, L., A randomized placebo-controlled trial of elafibranor in patients with primary biliary cholangitis and incomplete response to UDCA. *Journal of Hepatology*, 2021, 74.
18. Xiang, C., Chen, X., Yao, J., Yang, N., Yu, J., Qiu, Q., Zhang, S., Kong, X., Zhao, L., Fan, Z. C., Yu, P. and Teng, Y. O., Design, synthesis and anti-NASH effect evaluation of novel GFT505 derivatives in vitro and in vivo. *Eur J Med Chem*, 2023, 257, 1155-10.
19. Wang, P., Wang, Y., Liu, H., Han, X., Yi, Y., Wang, X. and Li, X., Role of triglycerides as a predictor of autoimmune hepatitis with cirrhosis. *Lipids Health Dis*, 2022, 21, 108.
20. Zhuge, Q., Zhang, Y., Liu, B. and Wu, M., Blueberry polyphenols play a preventive effect on alcoholic fatty liver disease C57BL/6 J mice by promoting autophagy to accelerate lipolysis to eliminate excessive TG accumulation in hepatocytes. *Ann Palliat Med*, 2020, 9, 1045-1054.
21. Shahi, A., Gautam, N., Rawal, S., Sharma, U. and Jayan, A., Lipid Profile and Ultrasonographic Grading in Alcoholic and Non Alcoholic Fatty Liver Patients. *Kathmandu Univ Med J (KUMJ)*, 2021, 19, 334-338.
22. Niu, A. and Qi, T., Diagnostic significance of serum type IV collagen (IVC) combined with aspartate aminotransferase (AST)/alanine aminotransferase (ALT) ratio in liver fibrosis. *Ann Transl Med*, 2022, 10, 1310.
23. Søren, N. and Fredrik, K., Determinants of VLDL-triglycerides production. *Current opinion in lipidology*, 2012, 23.
24. Naaziyah, A., Theresa, V. C. and Mandeep, K., Mechanistic Insights Delineating the Role of Cholesterol in Epithelial Mesenchymal Transition and Drug Resistance in Cancer. *Frontiers in Cell and Developmental Biology*, 2021, 9.
25. Wu, A. H., Biomarkers for cholesterol absorption and synthesis in hyperlipidemic patients: role for therapeutic selection. *Clin Lab Med*, 2014, 34, 157-166, viii.